Published in final edited form as:
Biochemistry. 2012 December 18; 51(50): 10066–10074. doi:10.1021/bi301394z.

Properties of Membrane-Incorporated WALP Peptides that are Anchored on Only One End†

Johanna M. Rankenberg[1], **Vitaly V. Vostrikov**[1], **Denise V. Greathouse**[1], **Christopher V. Grant**[2], **Stanley J. Opella**[2], and **Roger E. Koeppe II**[1,*]

[1]Department of Chemistry and Biochemistry, University of Arkansas, Fayetteville, AR 72701

[2]Department of Chemistry and Biochemistry, University of California, San Diego, La Jolla, CA 92093

Abstract

Peptides of the "WALP" family, acetyl-GWW$(LA)_n$LWWA-[ethanol]amide have proven to be opportune models for investigating lipid/peptide interactions. Because the average orientations and motional behavior of the N- and C-terminal Trp (W) residues differ, it is of interest to investigate how the positions of the tryptophans influence the properties of the membrane-incorporated peptides. To address this question, we synthesized acetyl-GGWW$(LA)_n$-ethanolamide and acetyl-$(AL)_n$WWG-ethanolamide, in which n = 4 or 8, which we designate as "N-anchored" and "C-anchored" peptides, respectively. Selected ^2H or ^{15}N labels were incorporated for solid-state NMR spectroscopy. These peptides can be considered "half"-anchored WALP peptides, having only one pair of interfacial Trp residues near either the amino or the carboxyl terminus. The hydrophobic lengths of the (n = 8) peptides are similar to that of WALP23. These longer half-anchored WALP peptides incorporate into lipid bilayers as α-helices, as reflected in their circular dichroism spectra. Solid-state NMR experiments indicate that the longer peptide helices assume defined transmembrane orientations with small non-zero average tilt angles, and moderate to high dynamic averaging in bilayer membranes of DOPC, DMPC and DLPC. The intrinsically small apparent tilt angles suggest that aromatic residue interactions with lipid head groups may play an important role in determining the magnitude of the peptide tilt in the bilayer membrane. The shorter (n = 4) peptides, in stark contrast to the longer peptides, display NMR spectra that are characteristic of greatly reduced motional averaging—probably due to peptide aggregation in the bilayer environment—and CD spectra that are characteristic of β-structure.

Keywords

deuterium and ^{15}N solid-state NMR; lipid bilayer; GALA analysis; PISEMA; tryptophan; peptide-lipid interaction; peptide dynamics

Model peptides have proven useful for describing the details of protein/lipid interactions in lipid bilayer membranes. For example, WALP and related peptides have been studied

†This work was supported in part by NSF grant MCB 0841227 and by the Arkansas Biosciences Institute. The peptide facility is supported by NIH grants RR31154 and RR16460. The NMR facilities are supported by NIH grant GM103450 and the Biotechnology Resource for NMR Molecular Imaging of Proteins at the University of California, San Diego, which is supported by NIH grant P41EB002031.

*Address correspondence to: 119 Chemistry Building, University of Arkansas, Fayetteville, AR 72701, Tel. (479) 575-4976; Fax. (479) 575-4049; rk2@uark.edu. .

SUPPORTING INFORMATION AVAILABLE. Additional NMR spectra, mass spectra, chromatogram, and Trp fluorescence spectra. This material is available free of charge via the Internet at http://pubs.acs.org.

extensively to determine their behavior and positioning in lipid bilayers of varying thickness. WALP peptides, originally developed using gramicidin A channels as inspiration (1), traditionally have contained two Trp residues on either side of a hydrophobic, helical core composed of alternating Leu and Ala residues, yielding the sequence pattern acetyl-GWWL$(AL)_n$WWA-amide (with "n" typically between 4.5 and 12). In proteins associated with biological membranes, such as photosynthetic reaction centers or potassium channels (2, 3), aromatic as well as charged amino acid side chains are often located at or near the membrane/water interfaces. The interfacial amino acid residues help to anchor the proteins in specific orientations within the bilayer. It follows that the aromatic Trp residues are key constituents of WALP model peptides, since they are the only residues available to restrict trans-bilayer movement or specify a particular tilt angle for the peptide helix (4).

Previous studies have addressed the concept of hydrophobic mismatch between WALP (or related peptides) and lipid bilayer membranes (4-6). The lipid bilayer thickness and the peptide hydrophobic length, defined as the distance between the Trp residues on either side of the Leu-Ala core, affect the lipid phase behavior and may influence the peptide orientation in cases where the bilayer phase is maintained. A remarkable and somewhat surprising recent finding (7) has revealed that peptides having only single Trp residues on both ends respond more systematically to changes in the lipid bilayer thickness than do peptides having pairs of Trp residues on both ends. Several methods have been employed to determine WALP or WALP-like peptide orientations within hydrated, oriented model lipid bilayer membranes. The measurements have included circular dichroism (CD) and infrared spectroscopy (1, 8), as well as solid-state NMR (4, 7, 9-11) and fluorescence quenching (12, 13), along with molecular modeling (9, 11, 14-16). The solid-state NMR methods have included the ^{2}H NMR-based Geometric Analysis of Labeled Alanines ("GALA") (4, 17) and the ^{15}N NMR-based Polarization Inversion with Spin Exchange at Magic Angle ("PISEMA") (18, 19). In several direct comparisons, the ^{15}N and ^{2}H methods have shown remarkable agreement (7, 10, 20). More recently, considerations of ensemble dynamics (21) or multiple parameters for treating dynamics have been incorporated into the analysis (7, 9, 14, 16, 20).

Here we describe the independent anchoring properties of Trp residues when present at only one end of a membrane-spanning peptide (Figure 1). Previous experiments have compared the influence of one and two Trp residue anchors (7), when present on both ends of a WALP or WALP-like peptide. The presence or absence of interfacial Trp residues in specific N-proximal or C-proximal positions has the potential to affect the peptide dynamics as well as the preferred helix orientation. The presence of Trp residue(s) on (only) one side of a membrane sequence, without any anchor residues on the other side, offers a means to investigate the properties of peptides that are "held" on only one end. For this purpose, we have developed "single-end" anchored WALP peptides, which we henceforth designate as "single-anchored." Each peptide incorporates one pair of Trp residues adjacent to a string of either 4 or 8 Leu-Ala repeating units, namely $(LA)_n$ in which "n" is 4 or 8. In this design, the C-anchored $(AL)_n$WWG and N-anchored GGWW$(LA)_n$ peptides each retain two Trp residues near one end (Figure 1). As is true for other WALP and GWALP peptides, the termini are blocked with acetyl and ethanolamide groups, so that charged ends are avoided.

Using CD and solid-state NMR methods, we have characterized the folding, orientation and dynamic properties of the single-end N- and C-anchored peptides, in DLPC, DMPC and DOPC bilayer membranes. The shorter $(LA)_4$-containing peptides were found to exhibit β structure and very slow dynamics, which we attribute to aggregation. For the $(LA)_8$-containing peptides well-resolved ^{2}H and ^{15}N NMR resonances are observed and enable a detailed analysis of peptide orientation and dynamics (20). Together the results provide useful comparisons with other membrane-spanning peptides that appear to be anchored on

only one side of a bilayer (22). We find that the N- or C-anchored peptides of sufficient length tend to span the bilayer as helices with small tilt angles and extensive dynamics. Shorter peptides, whose lengths are similar to the thickness of a lipid monolayer, seem not to span the half-bilayer leaflet but instead adopt β structure and aggregate.

MATERIALS AND METHODS

Materials

Isotope enriched amino acids (^{2}H and ^{15}N) and ^{2}H-depleted water were from Cambridge Isotope Laboratories (Andover, MA). Commercial L-alanine-d_4 was Fmoc-protected using Fmoc-ON-Succinimide as described (23). Unlabeled Fmoc-amino acids and preloaded Wang resin were obtained from Novabiochem (San Diego, CA) and Advanced Chemtech (Louisville, KY). Ethanolamine and trifluoroethanol (TFE) were from Sigma-Aldrich (St. Louis, MO). Lipids were obtained from Avanti polar lipids (Alabaster, AL). Other chemicals were the highest grade available from EMD (Gibbstown, NJ).

Peptides (Table 1) were synthesized as described previously (24). In some peptides, deuterium labeled alanine-d_4 was incorporated at specific positions in the sequence, namely in 100% abundance at a single residue, or at lower 50-75% abundance at another sequence position, by combining appropriate amounts of Fmoc-Ala-d_4 and Fmoc-Ala in one vial. In other peptides, ^{15}N-Leu and ^{15}N-Ala were incorporated at 100% isotope abundance in particular sequence positions. The isotope labeled amino acid positions are noted in the figure legends.

DLPC, DMPC and DOPC bilayer membrane lipids were chosen to represent a range of fluid bilayers of differing hydrophobic thickness, about 19.5, 23 and 27 Å, respectively (6, 25). The double bond in the acyl chains of DOPC is necessary to maintain appropriate lipid bilayer fluidity at physiological temperature. While the lipid unsaturation also will influence the lateral pressure profile (26), the influence of pressure or packing density appears rather minimal for the tilt angles of the types of helices considered here (6).

Vesicle samples containing 0.13 μM peptide and 7.8 μM lipid for CD spectroscopy were prepared by sonication, as previously described (7, 27). Spectra were recorded using a Jasco (Easton, MD) J710 CD spectropolarimeter, scanning 190-250 nm at 20 nm/min, using a 1 mm path length, 0.2 nm step resolution and 1 nm bandwidth, with five scans averaged. (Due to far UV absorption by the double bond in DOPC, samples in DOPC were scanned within 200-250 nm.) Samples for fluorescence spectroscopy were prepared by ~40-fold dilution of the samples used for CD spectroscopy. Intrinsic Trp emission spectra were recorded using a Perkin Elmer LS 55 fluorescence spectrophotometer, at an excitation wavelength of 284 nm, detection of emission in the 300-500 nm range, and slits of 7.5 nm for both excitation and emission. Ten scans recorded at a rate of 200 nm/min were averaged.

Samples for NMR spectroscopy were prepared as described previously (24). Glass plate samples had a peptide:lipid ratio of 1:40 and 45% hydration (w/w). Bicelle samples were prepared as described (24), using DMPC/DH-o-PC or DM-o-PC/DH-o-PC (for the ^{15}N labeled samples) in a molar ratio (q) of 3.2, and a ratio of ^{15}N-labeled peptide:DMPC of 1:80. Solid-state deuterium NMR spectra were recorded (24) at temperatures of 50 °C for the plate samples and 40 °C for the bicelle samples. High resolution separated local field solid-state NMR spectra obtained utilizing the SAMPI4 pulse sequence (28, 29) were obtained on a 500 MHz Bruker Avance spectrometer. Data were acquired using a 1 ms cross-polarization (CP) contact time, radio frequency (RF) field strengths of approximately 50 kHz; 54 t1 points were acquired in the indirect dimension, 8.0 ms of acquisition time in the direct (t2) dimension, and a 7.5 second recycle delay. ^{31}P NMR spectra (Figure S1 of the

Supporting Information) indicated that the lipids were well aligned. Combinations of ^{2}H quadrupolar splitting magnitudes, along with ^{15}N chemical shift and $^{15}N/^{1}H$ dipolar coupling values, when available, were used to describe the orientations and dynamics of the peptides in the different lipid systems (20). The methods for the semi-static and Gaussian treatments of the dynamics have been described (20, 24, 30).

RESULTS

The desired peptides in Table 1 were successfully synthesized and characterized. Mass spectra (Figure S2 of the Supporting Information) confirmed the expected isotopic mass distributions for labeled peptides with full or partial deuteration of two alanines. HPLC chromatograms (Figure S3 of the Supporting Information) revealed single major peaks, indicating that the synthetic peptides were ~95% pure.

The secondary structures of the membrane-incorporated peptides were examined by CD spectroscopy. The longer 19- or 20-residue peptides, with 8 Leu-Ala units, yield CD spectra characteristic of α-helices in DLPC, DMPC and DOPC (Figure 2). It is evident that the shorter lipids promote a larger extent of helix formation, perhaps due to better matching of the lipid and peptide hydrophobic lengths. The spectral differences could perhaps arise from partial helix unwinding in the longer lipids. We do not fully understand the reasons for these trends.

A much shorter 11-residue hydrophobic peptide, with Trp anchors at positions 9 and 10, which potentially could span a lipid monolayer as an α-helix, is not helical in any of the lipid bilayer membranes (Figure 2C). Instead the shorter C-anchored peptide, with its $(LA)_4$ sequence, exhibits CD spectra characteristic of a β-sheet in each of the lipid membranes. The deuterium NMR spectra additionally suggest that this shorter peptide undergoes aggregation. Indeed the spectra from hydrated, oriented DMPC bilayers with the 11-residue “half” WALP peptides show a characteristic Pake powder pattern, recognized as a full range of quadrupolar splittings that reaches a maximum at ~37 kHz (Figure 3E, F). The spectra are furthermore nearly identical for the $\beta = 0°$ and $\beta = 90°$ sample orientations, indicating slow motion of the peptide on the ^{2}H NMR timescale. The observed Pake patterns are likely a result of peptide aggregation. To address this issue, we synthesized a complementary N-anchored “half” WALP peptide having again only four Leu-Ala units (Table 1). When the N- and C-“half” WALP peptides were incorporated together in DMPC oriented bilayer samples, in a 1:1 ratio (1:40 total peptide:lipid), the resulting ^{2}H NMR spectra still remained as Pake patterns (Figure S4 of the Supporting Information). The preservation of the powder pattern indicates that the presence of the N-anchored “half” WALP peptide does not prevent aggregation of the C-anchored “half” WALP peptide. The N-anchored “half” WALP peptide furthermore exhibits CD spectra that suggest mixed secondary structures, albeit with evidence for some helix formation in DLPC (Figure 2D).

The longer WALP-like peptides, with pairs of Trp anchors on only the C-terminus or only the N-terminus, and with hydrophobic lengths sufficient to span lipid bilayers, do adopt transmembrane helical configurations in oriented DLPC, DMPC and DOPC lipid bilayers. The NMR spectra (Figure 3 A-D) display sharp, resolved ^{2}H resonances for the pairs of labeled alanines (Figure 3 A-D). Importantly, the narrow resonances and the factor of two reduction when changing the sample orientation from $\beta = 0°$ to $\beta = 90°$ indicate that these longer peptides undergo rapid motional averaging about the bilayer normal, in stark contrast to the aggregated shorter peptides that give essentially identical Pake patterns at $\beta = 0°$ and $\beta = 90°$ (Figure 3 E, F). Full sets of ^{2}H NMR spectra for both sample orientations are included as Figures S4-S8 of the Supporting Information. The quadrupolar splittings measured from the NMR spectra are summarized in Table 2, for the $\beta = 0°$ and $\beta = 90°$

sample orientations. Where possible, prior to the analysis of peptide orientation, the ^{2}H $\Delta\nu_q$ magnitudes observed at $\beta = 90°$ were multiplied by two and averaged with the values observed at $\beta = 0°$.

SAMPI4 solid-state NMR spectra were recorded for the bicelle-incorporated C-anchored "n=8" WALP peptide, labeled with ^{15}N in residues 5-15 (Figure 4A) or residues 11-15 (Figure 4B). The spectral patterns indicate an intermediate to large degree of peptide motion. Notably, the dispersion of the observed ^{15}N chemical shifts and ^{15}N/^{1}H dipolar couplings is much less than observed with AG^{2}ALWLALALALALALALWLAG^{22}A (GWALP23) (20, 30), yet conspicuously greater than observed for AW^{2}ALWLALALALALALALWLAW^{22}A ("WWALP23") (20). When five residues were labeled (Figure 4B), we could assign the magnitudes of the chemical shifts and dipolar couplings to specific residues. Assignments were based in part on the disposition of five consecutive residues in the framework of the helix geometry (24, 30), and in part on the agreement with observed ^{2}H quadrupolar splittings for equivalent residues. When eleven residues were labeled (Figure 4A), the substantial peak overlap precluded the assignment of individual resonances.

The ^{2}H quadrupolar splittings for the $\beta = 0°$ sample orientation, with uncertainties of about ±0.5 kHz, were used to calculate peptide average apparent tilt and direction of tilt (with respect to C of Gly^1 α) (4). Where available, the ^{15}N chemical shift and ^{15}N/^{1}H dipolar coupling values were also included. Molecular motions were treated in two ways, using either a semi-static approach, based on a single order parameter (4), or a Gaussian dynamics approach (16), based on the widths of distributions for the peptide tilt τ and helix azimuthal rotation ρ (defining the direction of tilt), expressed as σ_τ and σ_ρ, respectively. Results from both methods of analysis, using from 7 to 17 data points, show substantial agreement and are summarized in Table 4.

The Gaussian and semi-static methods for treating the dynamics enabled us to estimate the helix orientations and dynamic properties in bilayer membranes of DLPC, DMPC and DOPC, and in bicelles of DMPC/DH-o-PC. The orientations are described by the average tilt magnitude τ_o with respect to the bilayer normal and the average tilt direction (azimuthal rotation) ρ_o with respect to C_α of Gly^1 (Table 4). The dynamics are expressed by means of a principal order parameter S_{zz} (semi-static) or the widths of Gaussian distributions σ_τ and σ_ρ. The RMSD values, typically ~1.0 kHz, are in agreement with the precision of the experimental measurements. The Gaussian distributions σ_τ and σ_ρ were superimposed upon a fixed principal order parameter S_{zz} of 0.88, which is typical for representing an intrinsic molecular "wobble" for well oriented systems (1, 31). The semi-static calculations converged to lower principal order parameters (S_{zz}) between 0.65 and 0.8, which reflect some motional properties of the peptides in the different lipid membranes (Table 4).

Both the N-anchored and C-anchored WALP peptides, each with 8 Leu-Ala units, display small yet non-zero apparent average tilt angles in each of the lipid bilayer membranes (Table 4). While the precession entropy argues against a precisely zero tilt angle (15), the estimates for τ_o for all of the "single-anchored" peptide-lipid systems, as a group, fall within a narrow range of only 1°-13°. As expected, and as is observed generally with other systems (20, 32), when explicit parameters σ_τ and σ_ρ are considered, the Gaussian treatment of the peptide dynamics gives in most cases somewhat higher estimates of τ_o than does a semi-static treatment with only a single variable S_{zz} (Table 4). Even though one end of each peptide is without any obvious "anchor" residue, it is striking that in no case is τ_o estimated to be zero; which again, is disfavored by the precession entropy (15). Indeed, if τ_o would average to zero, then each of the alanine CD_3 quadrupolar splittings would average to the same value (see (4))—but such is not the case, as is evident in the GALA wave plots (Figure 5).

As estimates of the helix motions, the deduced values of σ_τ and σ_ρ indicate substantial dynamics for each peptide in all of the lipid systems (Table 4). The best fits for σ_ρ are generally ~60° and the best fits for σ_τ are generally ~20°. The minima in (σ_τ, σ_ρ) space are nevertheless shallow (Figure 6), indicating wide ranges of acceptable allowed combinations of (σ_τ, σ_ρ). As a corollary, the rather extensive peptide dynamics can be treated in a number of possible ways. If σ_τ and σ_ρ are not used, the (semi-static) variable S_{zz} falls into the range of 0.65-0.8 (Table 4), again indicating considerable dynamics for the "half-anchored" bilayer-spanning peptides.

The most probable helix azimuthal rotation, which defines the direction of tilt ρ_o, does not depend upon which method is used to estimate the dynamics (Table 4). For the N-anchored peptide, the preferred ρ_o does not change much with the lipid bilayer thickness (Figure 7A), although, as expected, ρ_o becomes essentially undefined as τ_o approaches zero, namely in the thicker DOPC. Also for the C-anchored peptide, for very small values of τ_o, the distribution of probable ρ values (Figure 7B) becomes either bimodal (DOPC) or very flat (DMPC).

The results for the C-anchored peptide in the DMPC bilayer and the bicelle environments (Table 4) agree very closely, with just marginally (2°-5°) higher estimates for τ_o in the bicelles. Notably, the assessments of σ_τ and σ_ρ, or alternatively of the variable S_{zz}, to represent the dynamics, are nearly identical between the DMPC bilayers and bicelles. We note also that the bicelle results are based on combinations of 17 data points that include ^{15}N chemical shifts and $^{15}N/^{1}H$ dipolar couplings in addition to ^{2}H quadrupolar couplings. Nevertheless, the fitted PISA wheel patterns (Figure 4A) depend very little on whether the $^{15}N/^{1}H$ data are analyzed alone or in combination with ^{2}H data. In either case, the peptide dynamics and dispersion of resonances around the PISA wheel are intermediate between the cases of minimal (GWALP23) or very extensive (WWALP23) dynamic averaging of the NMR observables (7, 20).

The NMR experiments were complemented by measurements of the intrinsic Trp fluorescence spectra (Figure S9 of the Supporting Information). The emission maxima are 340 nm for the N-anchored (n = 8) WALP and 345 nm for the C-anchored (n = 8) peptide, compared to ~351 nm expected for Trp in an entirely aqueous environment. Each spectrum reports an average environment for the two Trp residues in a particular peptide. No change in λ_{max} with lipid thickness was observed for either of the peptides, suggesting that the pair of adjacent Trp residues on one side of the transmembrane helix may "float" to a preferred location within the bilayer/solution interface. The spectra suggest furthermore that the Trp residues of the N-anchored peptide, blue-shifted with respect to those of the C-anchored peptide, occupy average positions that are slightly more sequestered from the aqueous environment.

DISCUSSION

Traditional WALP peptides contain two Trp residues on either side of a Leu-Ala helical core of variable length, $(LA)_n$. Because the orientational preferences and motional behavior of the N- and C-terminal Trp residues can be different (33), we developed peptides with two Trp residues on only one side of a $(LA)_n$ sequence which, since anchored on only one end, becomes effectively a "tail" sequence instead of a "core" sequence. The "half"-anchored WALP peptides of various lengths allowed us to address questions about the lipid interactions of the $(LA)_n$ tail sequences, including issues of secondary structure, aggregation behavior, potential for transmembrane topology, helix tilt and dynamics. It is noteworthy that strikingly different behavior was observed for the shorter (n = 4) peptides as opposed to the longer (n = 8) peptides in lipid bilayer membranes.

For the shorter peptides with the $(LA)_4$ tail sequence, we observe neither a helical conformation nor a leaflet-spanning orientation. The results for a-ALALALALWWG-e and a-GGWWLALALALA-e (Table 1) are in agreement with the β-structure and aggregation observed previously for a-WLLLLL in POPC bilayer membranes (34, 35). Indeed, for the shorter $(LA)_4$ peptides, the CD spectra (Figure 2) indicate β-structure; and the NMR spectra (Figure 3) indicate restricted motion, consistent with peptide aggregation. Consequently, for peptides that are too short to span a bilayer, in both the ALALALALWWG and WLLLLL families, it appears that the formation of β-structure is related to aggregation. Some sequence changes, for example WLWLL, inhibit both the aggregation and the β-structure (34). Longer $(AL)_n$ peptides that are able to adopt the transmembrane topology, so as to span the bilayer, also fold into α-helices (Figure 2). Interestingly, correlations between secondary structure and protein aggregation furthermore relate to a variety of neurodegenerative diseases (36-39).

The longer half-anchored WALP peptides, those with $(LA)_8$ core sequences, have hydrophobic lengths similar to those of WALP19 or WALP23 (1, 40), but are anchored to the lipid bilayer interface region on only one side. They incorporate into lipid bilayers as transmembrane helices and, unlike the shorter analogues, show no signs of aggregation. It is of interest to compare the average tilt and dynamics of uncharged transmembrane helices that possess either: (a) two interfacial Trps on both ends (4, 7, 9, 17, 32, 41), (b) only one interfacial Trp on both ends (6, 7, 20) or (c) two interfacial Trps on only one end (this work). These categories of transmembrane helical peptides have been examined in detail in bilayer membrane of different thickness, DOPC, DMPC and DLPC.

When two interfacial Trps are present on both ends of a transmembrane helix, a prominent feature is extensive dynamic averaging of NMR observables (9, 14, 20), which consequently do not change much with the membrane thickness (4, 17, 32). Remarkably, with fewer tryptophans, namely only one Trp on each end of a core transmembrane helix, the dynamic averaging is reduced rather dramatically, and the NMR observables show systematic variation with the membrane thickness, such that the apparent helix tilt scales quite nicely with the membrane thickness (6, 7, 20). A similar core helix flanked by a single Tyr and a single Trp shows a similarly low level of dynamic averaging (27); nevertheless, the incorporation of just one more tyrosine on one end restores the extensive dynamic behavior (27).

Within this context of single versus multiple interfacial aromatic residues flanking a central transmembrane helix, the “half-anchored” WALP peptides with the $(LA)_8$ tails introduce a new category. With one end now devoid of any aromatic residues, the result once again is dynamic averaging along with only small variations with the membrane thickness. Indeed the bilayer thickness dependence of the NMR observables—in DOPC, DMPC and DLPC lipid bilayer membranes—appears to be similar yet somewhat smaller than for WALP23 (17). The scenario that the “half-anchored” $(LA)_8$ WALP peptides are tilted very little and/or experience extensive motional averaging can be rationalized by both the lack of anchoring residues on one side and the multiple interfacial tryptophans on the other side of the lipid membrane. In any case, it is reasonable that, with one end “free,” neither N-terminal nor C-terminal anchoring (alone) should be expected to generate a large helix tilt within a lipid bilayer. Interestingly, the most probable azimuthal rotation angle ρ_o (defining the direction of tilt) in DLPC is roughly opposite for the C- and N-anchored $(LA)_8$-containing peptides. As anticipated, when the tilt magnitude approaches zero, the preferred azimuthal rotation defining the tilt direction becomes undefined (see Figure 7).

It is of particular interest to compare the dynamic behavior of a-ALALALALALALALALWWG-e (Figure 4) with that of a-

AWALWLALALALALALALWLAWA-e (WWALP23) (20). Comparing the respective $^{15}N/^{1}H$ dipolar couplings and 15N chemical shifts, it is apparent that ALALALALALALALALWWG exhibits intermediate dynamic behavior, in between that of the highly dynamic WWALP23 and the much less dynamic AGALWLALALALALALALWLAGA (GWALP23). Indeed, for GWALP23 the backbone $^{15}N/^{1}H$ dipolar couplings and ^{15}N chemical shifts appear as fully dispersed individual resonances, for WWALP23 they collapse to a single peak (20), and for ALALALALALALALALWWG the backbone ^{15}N observables show the intermediate case of partial overlap (Figure 7). The dynamic properties of the membrane-spanning helices are regulated by the numbers and locations of interfacial tryptophan (and tyrosine) residues.

The results for analysis of helix tilt in magnetically oriented bicelles of DMPC/DH-o-PC and in mechanically oriented DMPC bilayers show close agreement (Table 4). Whether a combined analysis of deuterium and $^{15}N/^{1}H$ observables (17 data points) for the bicelles or an analysis of only the deuterium $\Delta\nu_q$ magnitudes (7 data points) for the bilayers is utilized, both systems yield outcomes of 55-60° for σ_ρ and ~18° for σ_τ, along with similar almost vanishingly small values for τ_o (Table 4). For this example, therefore, the DMPC-based bilayer and bicelle systems show agreement.

The WALP-like peptides having double Trp anchors on only one end provide new insights into the anchoring behavior of Trp residues and the importance of peptide hydrophobic length. The ^{2}H NMR and ^{15}N NMR experiments indicate small tilt angles and extensive dynamics for the longer bilayer-spanning helical peptides with the $(LA)_8$ tails. The properties of the N- and C-anchored peptides are similar. As expected, the direction of the peptide tilt becomes essentially undefined when the tilt magnitude becomes very small. The shorter half-WALP peptides with $(LA)_4$ tails form aggregates having β-type secondary structure.

Supplementary Material

Refer to Web version on PubMed Central for supplementary material.

Acknowledgments

We thank Patrick van der Wel, James Hinton and Marvin Leister for helpful discussions.

ABBREVIATIONS

CD	circular dichroism
DH-o-PC	1,2-di-O-hexylphosphatidylcholine
DLPC	1,2-dilauroylphosphatidylcholine
DMPC	1,2-dimyristoylphosphatidylcholine
DM-o-PC	1,2-di-O-myristoylphosphatidylcholine
DOPC	1,2-dioleoylphosphatidylcholine
Fmoc	Fluorenylmethoxycarbonyl
GALA	Geometric analysis of labeled alanines
MtBE	methyl-*t*-butyl ether
PISEMA	Polarization inversion with spin exchange at magic angle

POPC	1-palmitoyl, 2-oleoyl-phosphatidylcholine
TFA	trifluoroacetic acid

REFERENCES

1. Killian JA, Salemink I, dePlanque MRR, Lindblom G, Koeppe RE II, Greathouse DV. Induction of nonbilayer structures in diacylphosphatidylcholine model membranes by transmembrane alpha-helical peptides: Importance of hydrophobic mismatch and proposed role of tryptophans. Biochemistry. 1996; 35:1037–1045. [PubMed: 8547239]
2. Schiffer M, Chang CH, Stevens FJ. The functions of tryptophan residues in membrane proteins. Protein Eng. 1992; 5:213–214. [PubMed: 1409540]
3. Doyle DA, Morais Cabral J, Pfuetzner RA, Kuo A, Gulbis JM, Cohen SL, Chait BT, MacKinnon R. The structure of the potassium channel: molecular basis of K+ conduction and selectivity. Science. 1998; 280:69–77. [PubMed: 9525859]
4. van der Wel PCA, Strandberg E, Killian JA, Koeppe RE II. Geometry and intrinsic tilt of a tryptophan-anchored transmembrane alpha-helix determined by ^{2}H NMR. Biophys. J. 2002; 83:1479–1488. [PubMed: 12202373]
5. de Planque MR, Boots JW, Rijkers DT, Liskamp RM, Greathouse DV, Killian JA. The effects of hydrophobic mismatch between phosphatidylcholine bilayers and transmembrane alpha-helical peptides depend on the nature of interfacially exposed aromatic and charged residues. Biochemistry. 2002; 41:8396–8404. [PubMed: 12081488]
6. Vostrikov VV, Koeppe RE II. Response of GWALP transmembrane peptides to changes in the tryptophan anchor positions. Biochemistry. 2011; 50:7522–7535. [PubMed: 21800919]
7. Vostrikov VV, Daily AE, Greathouse DV, Koeppe RE II. Charged or aromatic anchor residue dependence of transmembrane peptide tilt. J. Biol. Chem. 2010; 285:31723–31730. [PubMed: 20667827]
8. de Planque MR, Goormaghtigh E, Greathouse DV, Koeppe RE 2nd, Kruijtzer JA, Liskamp RM, de Kruijff B, Killian JA. Sensitivity of single membrane-spanning alpha-helical peptides to hydrophobic mismatch with a lipid bilayer: effects on backbone structure, orientation, and extent of membrane incorporation. Biochemistry. 2001; 40:5000–5010. [PubMed: 11305916]
9. Ozdirekcan S, Etchebest C, Killian JA, Fuchs PF. On the orientation of a designed transmembrane peptide: toward the right tilt angle? J. Am. Chem. Soc. 2007; 129:15174–15181. [PubMed: 18001020]
10. Vostrikov VV, Grant CV, Daily AE, Opella SJ, Koeppe RE 2nd. Comparison of “Polarization inversion with spin exchange at magic angle” and “geometric analysis of labeled alanines” methods for transmembrane helix alignment. J. Am. Chem. Soc. 2008; 130:12584–12585. [PubMed: 18763771]
11. Vostrikov VV, Hall BA, Greathouse DV, Koeppe RE 2nd, Sansom MS. Changes in transmembrane helix alignment by arginine residues revealed by solid-state NMR experiments and coarse-grained MD simulations. J. Am. Chem. Soc. 2010; 132:5803–5811. [PubMed: 20373735]
12. Sparr E, Ash WL, Nazarov PV, Rijkers DT, Hemminga MA, Tieleman DP, Killian JA. Self-association of transmembrane alpha-helices in model membranes: importance of helix orientation and role of hydrophobic mismatch. J. Biol. Chem. 2005; 280:39324–39331. [PubMed: 16169846]
13. Holt A, Koehorst R, Rutters-Meijneke T, Gelb M, Rijkers D, Hemminga MA, Killian JA. Tilt and rotation angles of a transmembrane model peptide as studied by fluorescence spectroscopy. Biophys. J. 2009; 97:2258–2266. [PubMed: 19843458]
14. Esteban-Martin S, Salgado J. The dynamic orientation of membrane-bound peptides: bridging simulations and experiments. Biophys. J. 2007; 93:4278–4288. [PubMed: 17720729]
15. Lee J, Im W. Transmembrane helix tilting: insights from calculating the potential of mean force. Phys. Rev. Lett. 2008; 100:018103. [PubMed: 18232823]

16. Strandberg E, Esteban-Martin S, Salgado J, Ulrich AS. Orientation and dynamics of peptides in membranes calculated from 2H-NMR data. Biophys. J. 2009; 96:3223–3232. [PubMed: 19383466]
17. Strandberg E, Ozdirekcan S, Rijkers DT, van der Wel PC, Koeppe RE 2nd, Liskamp RM, Killian JA. Tilt angles of transmembrane model peptides in oriented and non-oriented lipid bilayers as determined by 2H solid-state NMR. Biophys. J. 2004; 86:3709–3721. [PubMed: 15189867]
18. Wang J, Denny J, Tian C, Kim S, Mo Y, Kovacs F, Song Z, Nishimura K, Gan Z, Fu R, Quine JR, Cross TA. Imaging membrane protein helical wheels. J. Magn. Reson. 2000; 144:162–167. [PubMed: 10783287]
19. Marassi FM, Opella SJ. A solid-state NMR index of helical membrane protein structure and topology. J. Magn. Reson. 2000; 144:150–155. [PubMed: 10783285]
20. Vostrikov VV, Grant CV, Opella SJ, Koeppe RE II. On the combined analysis of ^{2}H and $^{15}N/^{1}H$ solid-state NMR data for determination of transmembrane peptide orientation and dynamics. Biophys. J. 2011; 101:2939–2947. [PubMed: 22208192]
21. Kim T, Jo S, Im W. Solid-State NMR Ensemble Dynamics as a Mediator between Experiment and Simulation. Biophys. J. 2011; 100:2922–2928. [PubMed: 21689525]
22. Percot A, Zhu XX, Lafleur M. Design and characterization of anchoring amphiphilic peptides and their interactions with lipid vesicles. Biopolymers. 1999; 50:647–655. [PubMed: 10508967]
23. ten Kortenaar PBW, Van Dijk BG, Peeters JM, Raaben BJ, Adams PJHM, Tesser GI. Rapid and efficient method for the preparation of Fmoc-amino acids starting form 9-fluorenylmethanol. Int. J. Pept. Prot. Res. 1986; 27:398–400.
24. Rankenberg JM, Vostrikov VV, DuVall CD, Greathouse DV, Koeppe RE II, Grant CV, Opella SJ. Proline kink angle distributions for GWALP23 in lipid bilayers of different thicknesses. Biochemistry. 2012; 51:3554–3564. [PubMed: 22489564]
25. de Planque MRR, Greathouse DV, Koeppe RE, Schafer H, Marsh D, Killian JA. Influence of lipid/peptide hydrophobic mismatch on the thickness of diacylphosphatidylcholine bilayers. A H-2 NMR and ESR study using designed transmembrane alpha-helical peptides and gramicidin A. Biochemistry. 1998; 37:9333–9345. [PubMed: 9649314]
26. Binder H, Gawrisch K. Effect of unsaturated lipid chains on dimensions, molecular order and hydration of membranes. Journal of Physical Chemistry B. 2001; 105:12378–12390.
27. Gleason NJ, Vostrikov VV, Greathouse DV, Grant CV, Opella SJ, Koeppe RE II. Tyrosine replacing tryptophan as an anchor in GWALP peptides. Biochemistry. 2012; 51:2044–2053. [PubMed: 22364236]
28. Nevzorov AA, Opella SJ. A “magic sandwich” pulse sequence with reduced offset dependence for high-resolution separated local field spectroscopy. J. Magn. Reson. 2003; 164:182–186. [PubMed: 12932472]
29. Nevzorov AA, Opella SJ. Selective averaging for high-resolution solid-state NMR spectroscopy of aligned samples. J. Magn. Reson. 2007; 185:59–70. [PubMed: 17074522]
30. Gleason NJ, Greathouse DV, Koeppe RE II. Using Tyrosine to Anchor a Transmembrane Peptide. Biophys. J. 2011; 100:635a–636a. (abstract).
31. Pulay P, Scherer EM, van der Wel PCA, Koeppe RE. Importance of tensor asymmetry for the analysis of ^{2}H NMR spectra from deuterated aromatic rings. J. Am. Chem. Soc. 2005; 127:17488–17493. [PubMed: 16332101]
32. Strandberg E, Esteban-Martin S, Ulrich AS, Salgado J. Hydrophobic mismatch of mobile transmembrane helices: Merging theory and experiments. Biochim. Biophys. Acta. 2012; 1818:1242–1249. [PubMed: 22326890]
33. van der Wel PC, Reed ND, Greathouse DV, Koeppe RE 2nd. Orientation and motion of tryptophan interfacial anchors in membrane-spanning peptides. Biochemistry. 2007; 46:7514–7524. [PubMed: 17530863]
34. Wimley WC, Hristova K, Ladokhin AS, Silvestro L, Axelsen PH, White SH. Folding of beta-sheet membrane proteins: A hydrophobic hexapeptide model. Journal of Molecular Biology. 1998; 277:1091–1110. [PubMed: 9571025]
35. Wimley WC, White SH. Reversible unfolding of beta-sheets in membranes: A calorimetric study. Journal of Molecular Biology. 2004; 342:703–711. [PubMed: 15342231]

36. Bates G. Huntingtin aggregation and toxicity in Huntington's disease. Lancet. 2003; 361:1642–1644. [PubMed: 12747895]

37. Fawzi NL, Yap EH, Okabe Y, Kohlstedt KL, Brown SP, Head-Gordon T. Contrasting disease and nondisease protein aggregation by molecular simulation. Acc. Chem Res. 2008; 41:1037–1047. [PubMed: 18646868]

38. Carulla N, Zhou M, Giralt E, Robinson CV, Dobson CM. Structure and Intermolecular Dynamics of Aggregates Populated during Amyloid Fibril Formation Studied by Hydrogen/Deuterium Exchange. Acc. Chem Res. 2010; 43:1072–1079. [PubMed: 20557067]

39. Stanley CB, Perevozchikova T, Berthelier V. Structural formation of huntingtin exon 1 aggregates probed by small-angle neutron scattering. Biophys. J. 2011; 100:2504–2512. [PubMed: 21575585]

40. de Planque MRR, Kruijtzer JAW, Liskamp RMJ, Marsh D, Greathouse DV, Koeppe RE, de Kruijff B, Killian JA. Different membrane anchoring positions of tryptophan and lysine in synthetic transmembrane alpha-helical peptides. Journal of Biological Chemistry. 1999; 274:20839–20846. [PubMed: 10409625]

41. Holt A, Rougier L, Reat V, Jolibois F, Saurel O, Czaplicki J, Killian JA, Milon A. Order parameters of a transmembrane helix in a fluid bilayer: case study of a WALP peptide. Biophys. J. 2010; 98:1864–1872. [PubMed: 20441750]

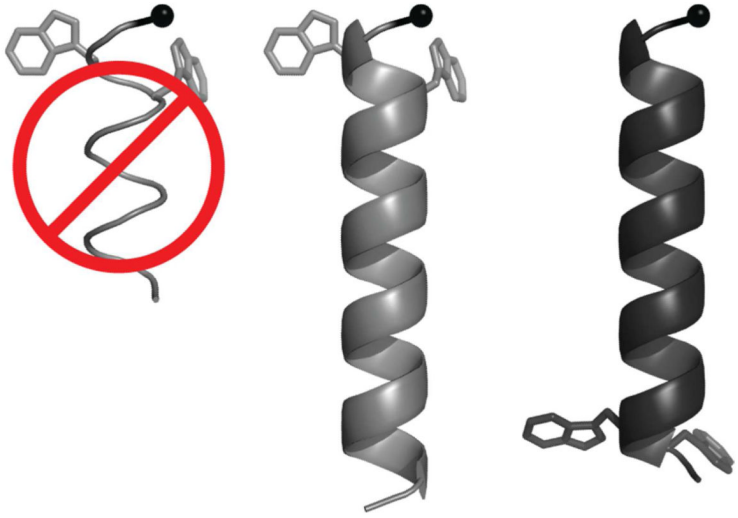

Figure 1.
Schematic ribbon models for hydrophobic peptides of length 11 residues or 19 residues, with two Trp residues near the N-terminal (lighter gray) or near the C-terminal (darker gray). The longer peptides could span a lipid bilayer membrane as α-helices, whereas the shorter peptides could span only about one leaflet of a bilayer. Nevertheless, the shorter peptides are not helical under such conditions.

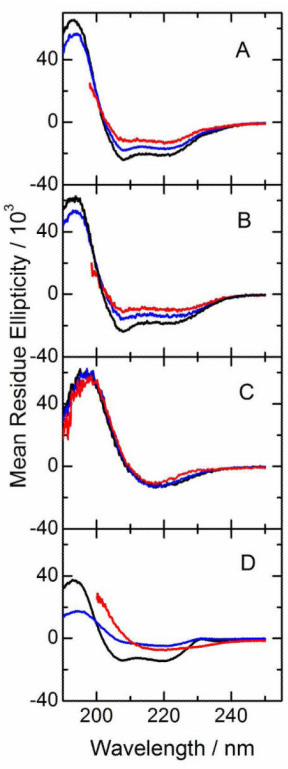

Figure 2.
Circular dichroism spectra of N-anchored “n=8” (A), C-anchored “n=8” (B), C-anchored “n=4” (C), and N-anchored “n=4” (D) WALP peptides, in vesicles of DLPC (black), DMPC (blue) or DOPC (red). It is evident that the shorter lipids promote a larger extent of α-helix formation for the longer peptides.

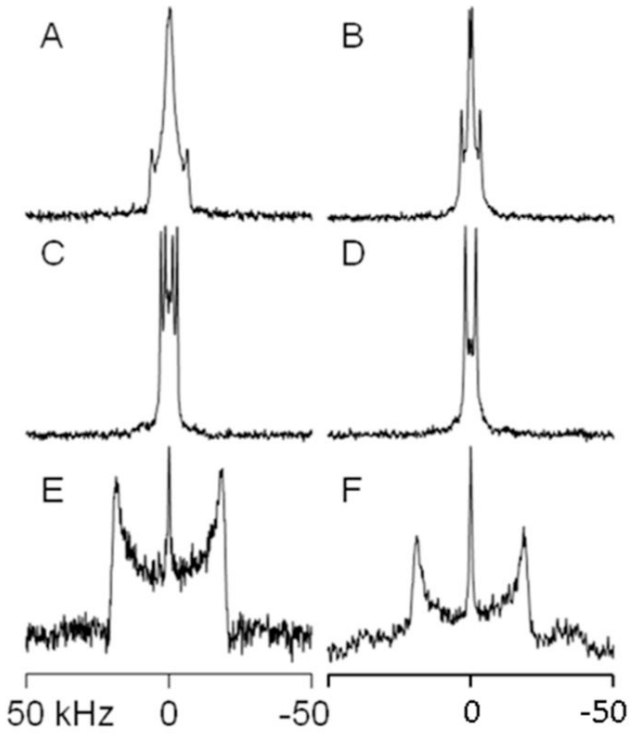

Figure 3.

^{2}H NMR spectra of labeled alanines in N-anchored “n=8” (A, B), C-anchored “n=8” (C, D) and C-anchored “n=4” (E, F) WALP peptides, in hydrated bilayers of DMPC oriented at β = 0° (A, C, E) or β = 90° (B, D, F); temperature 50 °C. The ^{2}H-labeled alanine residues and % deuteration are A^6 and A^8 70% 100% (A, B); or A^{13} and A^{15} 70% 100% (C, D); or A^3 and A^5 75% 50% and $A^7_{100\%}$ (E, F).

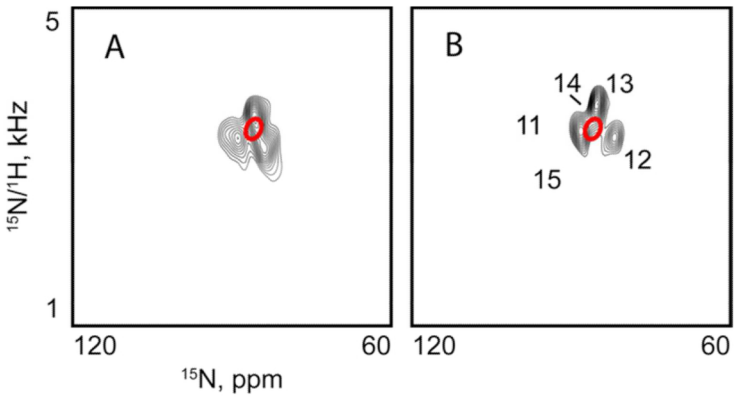

Figure 4.

SAMPI4 spectra for C-anchored “n=8” WALP peptide with ^{15}N-labels in residues 5-15 (A), or in residues 11-15 (B). Peak assignments for labeled residues are shown in B. The PISA wheel patterns are based on analysis of a combination of ^{2}H and ^{15}N data, with equal weights for the ^{2}H quadrupolar couplings, ^{15}N/^{1}H dipolar couplings and ^{15}N chemical shifts.

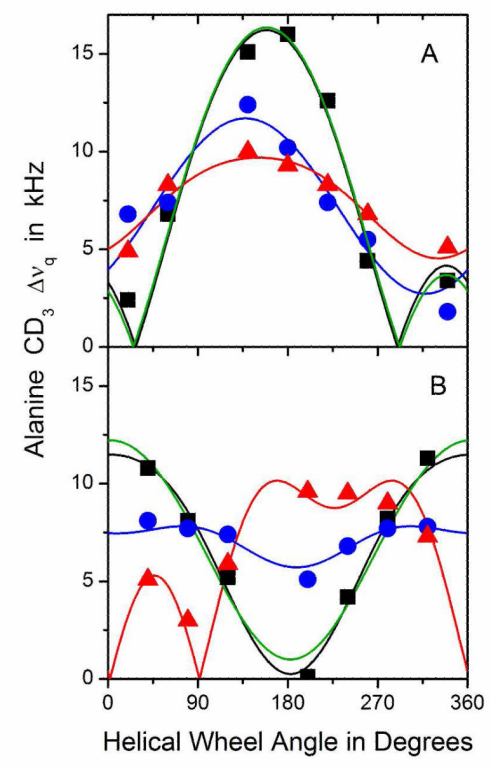

Figure 5.

GALA quadrupolar wave plots for “half-anchored” “n=8” WALP peptides, with the paired Trp anchor residues that are N-proximal (A), or C-proximal (B). The curves represent the fits using Gaussian dynamics in the lipid environments of DLPC (black), DMPC (blue) or DOPC (red). For comparison, the semi-static fits are shown as green curves in DLPC.

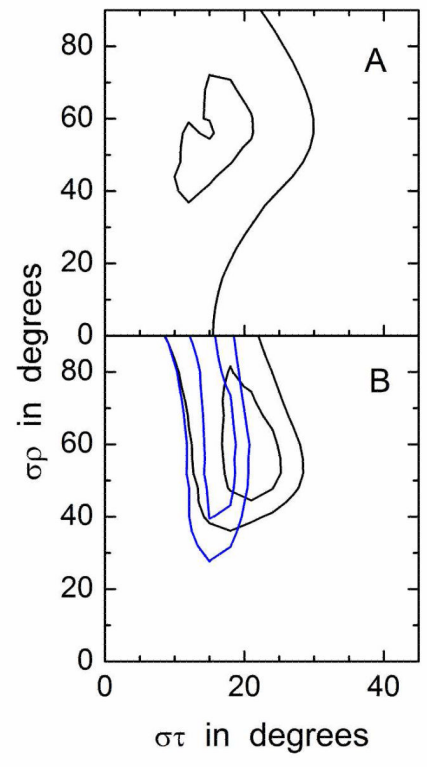

Figure 6.
Gaussian dynamics. RMSD (στ, σρ) graphs for the Gaussian dynamics analysis of the "n=8" N-anchored (A) and C-anchored (B) WALP peptides in mechanically oriented bilayers of DLPC (black), or in magnetically oriented bicelles (blue). The contour levels are 1.0 and 2.0 kHz.

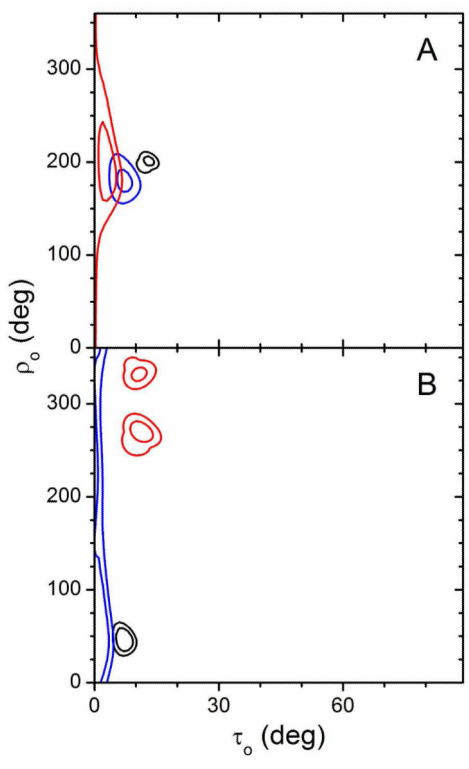

Figure 7.

Orientations of half-anchored peptides. RMSD plots for the apparent tilt of the “n=8” N-anchored (A) and C-anchored (B) WALP peptides in oriented bilayers of DLPC (black), DMPC (blue) or DOPC (red). RMSD is plotted as a function of τ and ρ values for the optimum values of σ_τ and σ_ρ in Gaussian calculations (see Table 4 and Figure 5). Contours are drawn at 1.2 kHz and 2.0 kHz.

Table 1

Sequences of peptides[a]

C-anchored WALP	n=4[b]	a-ALALALALWWG-e
C-anchored WALP	n=8[b]	a-ALALALALALALALWWG-e
N-anchored WALP	n=8[b]	a-GGWWLALALALALALALALA-e
N-anchored WALP	n=4[b]	a-GGWWLALALALA-e

[a]The abbreviations “a” and “e” denote acetyl and ethanolamide, respectively. Labels were incorporated for ^{2}H and ^{15}N NMR experiments, as indicated in Methods.

[b]The integer “n” denotes the number of (LA) or (AL) dipeptide units in the sequence.

Table 2

Observed ^{2}H quadrupolar splitting magnitudes (kHz) for labeled alanine methyl groups in half-anchored WALP peptides[a]

	N-anchored WALP			
Ala[b]	**DLPC**	**DMPC**	**bicelles[c]**	**DOPC**
6	15.1	12.4	--	10.0
8	3.4	1.8	--	5.1
10	16.0	10.2	--	9.3
12	2.4	6.8	--	4.9
14	12.6	7.4	--	8.3
16	6.8	7.4	--	8.3
18	4.4	5.5	--	6.8
	C-anchored WALP			
3	0.0	5.1	0.0	9.6
5	10.8	8.1	10.6	5.1
7	4.2	6.8	4.0	9.5
9	7.9	7.7	7.4	3.0
11	7.9	7.7	7.4	9.0
13	5.2	7.4	6.2	5.9
15	11.3	7.4	8.8	7.4

[a] Values in kHz for the $\beta = 0°$ sample orientation in the indicated lipid bilayers or in bicelles. Signals are from the CD_3 side chain.

[b] Position of alanine residue in the sequence.

[c] Bicelles composed of DMPC/DH-o-PC (q = 3.2). Values left blank were not measured.

Table 3

Dipolar couplings and ^{15}N chemical shift values for $^{15}N/^{1}H$ groups in C-anchored (n=8) WALP peptide in DM-o-PC/DH-o-PC bicelles (q = 3.2)[a]

Residue	$^{15}N/^{1}H$ dipolar coupling, kHz	^{15}N chemical shift, ppm
11	3.55	88.8
12	3.35	82.2
13	3.85	85.5
14	3.70	86.5
15	3.30	87.0

[a]Values are listed for bicelle samples, corresponding to a β = 90° sample orientation.

Table 4

Calculated orientations of N-anchored and C-anchored WALP peptides in lipid bilayers and bicelles[a]

Trp positions[b]	Lipid	Model	τ_0	σ_τ	ρ_0	σ_ρ	S_{zz}	RMSD	n[c]
N-anchor	DLPC	Gaussian	13°	18°	201°	60°	0.88[d]	0.9 kHz	7
	DLPC	semi-static	7°	n.a.[e]	202°	n.a.[e]	0.75	0.9	7
	DMPC	Gaussian	7°	15°	180°	76°	0.88[d]	0.9	7
	DMPC	semi-static	3°	n.a.[e]	180°	n.a.[e]	0.78	0.9	7
	DOPC	Gaussian	3°	15°	193°	60°	0.88[d]	0.5	7
	DOPC	semi-static	2°	n.a.[e]	204°	n.a.[e]	0.78	0.8	7
C-anchor	DLPC	Gaussian	7°	21°	46°	56°	0.88[d]	0.5	7
	DLPC	semi-static	4°	n.a.[e]	46°	n.a.[e]	0.73	0.6	7
	DMPC	Gaussian	1°	18°	52°	56°	0.88[d]	0.4	7
	DMPC	semi-static	1°	n.a.[e]	60°	n.a.[e]	0.77	0.6	7
	Bicelles	Gaussian	8°	18°	56°	86°	0.88[d]	0.9	17[f]
	Bicelles	semi-static	3°	n.a.[e]	55°	n.a.[e]	0.74	0.9	17[f]
	DOPC	Gaussian	11°	33°	270°	44°	0.88[d]	0.6	7
	DOPC	semi-static	2°	n.a.[e]	285°	n.a.[e]	0.67	1.0	7

[a] The Gaussian model for the dynamics uses a fixed principal order parameter S_{ZZ} (16), representing the dynamic extent of (mis)alignment (angle α) between the molecular *z*-axis and its average orientation, characterized by the time average $S_{ZZ} = \langle 3\cos^2\alpha - 1\rangle/2$ (31). Within this context, further motions can be characterized by the widths σ_τ and σ_ρ of Gaussian distributions about the average values of tilt magnitude τ_0 and tilt direction ρ_0 (16). An alternative semi-static analysis, using three parameters instead of four, determines the best fit (lowest RMSD) as a function of τ_0, ρ_0 and S_{ZZ}.

[b] Each peptide has 8 repeating (Leu-Ala) units. See sequences in Table 1.

[c] The number of data points for the calculation is seven ^{2}H methyl quadrupolar couplings, unless otherwise noted.

[d] Fixed value.

[e] Not applicable.

[f] In the bicelles of DMPC/DH-o-PC (q = 3.2), the data points consisted of seven ^{2}H methyl quadrupolar couplings, five ^{1}H-^{15}N dipolar couplings and five ^{15}N chemical shifts. Data points weighted equally.